



Characteristics and Morphological Studies of Nd Doped Titanium Thin Film Coating on SS 316L by DC Sputtering

Hiba A. Abdullah, Rana A. Anae *

Department of Materials Engineering, University of Technology, Baghdad, Iraq

ARTICLE INFO

Article history:

Received June 11, 2022

Accepted July 15, 2022

Keywords:

Nd

Titanium coating

Bioimplant

DC sputtering

SS 316L

ABSTRACT

Nd doped Titanium coating was applied on stainless steel 316L by DC sputtering method to investigate the corrosion behavior in simulated body fluid at 37°C. The characterization of coated surface was done by XRD analysis that shows the incorporation of coating peaks within peaks of substrate (SS 316L), SEM/EDS also used to identify the structure and elemental composition of coating layer and the results indicated the formation of titanium carbide with neodymium particles which distributed on the titanium thin film and the EDS analysis showed the presence of Ti, Nd, O and high percent of C. AFM analysis indicated the increasing in surface roughness from 52.20 nm to 176.7 nm after coating with more valleys and peaks in two and three dimensions images, as well as more resistant for wear after coating from Abbott-Firestone results. The results of corrosion measurement showed the more positive corrosion potential for coated surface and decreasing in corrosion current density to obtain protection efficiency equal to 97.11% due to ability of the coating layer to isolate the substrate from corrosive environment.

1. Introduction

There are many ways used to reduce corrosion damage, but in bioapplications, the coatings are the alternate methods to reduce corrosion and provide the biocompatibility. Surface modification and ion implantation by protective biocoatings were applied by different techniques including electrodeposition, diffusion process, physical vapour deposition, cladding, and chemical vapour deposition and etc. The selected material for coating is important to ensure the lowest level of toxicity, therefore titanium has attention to use as coating in different ways, Sofiane et al. studied the carbon doped titanium nitride coating by DC sputtering for bio application [1]. Austenitic stainless steels (especially SS 316L) is the almost used material for implantation because of ease of fabrication, lower cost, and welding as

compared to $Co - Cr$ alloys and Ti and its alloys, but there are more than 90% of the failure for implantation can occur because of crevice and corrosion attack. Therefore, the coating is the best method for reducing corrosion problem with thin film as produced by DC sputtering technique.

Fouada et al. prepared $Ti - O$, $Ti - O - C$ and $Ti - O - C - N$ films using tetrabutyl orthotitanate as a precursor by chemical vapor deposition (CVD) technique in presence of different gases, where titanium nitride (Ti_2N and TiN) phases, TiO_2 and TiC phases were formed [2], Linus et al. applied titanium carbonitride ($Ti(C, N)$) films by CVD technique [3] and Barbara et al. studied the development of multifunctional biomedical (TiO_2) coatings doubly-doped with Ag and Ca ions by dip-coating method on steel to investigate many

* Corresponding author.

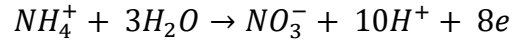
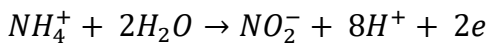
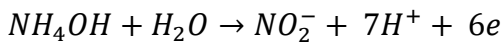
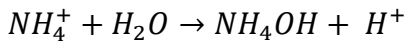
E-mail address: dr.rana_afif@yahoo.com

DOI: [10.24237/djes.2022.15303](https://doi.org/10.24237/djes.2022.15303)



biological properties and corrosion [4] as well as using niobium oxide [5] and ceria by RF sputtering [6, 7].

In present work, Nd (NO₃)₃ was doped with titanium to apply coating on SS 316 L by DC sputtering method due to the role of neodymium and nitrogen in reducing corrosion. Where neodymium (Nd) compounds have a moderate to low toxicity and it represents an anticoagulant. In the other hand, the presence of nitrogen improves the corrosion resistance because of the formation of ammonium ions at the pit sites and the ammonium ions such as NH₄⁺ and NO₃⁻ increase the pH at the surface that work to reduce growth kinetics at metal/film interface, and then the inhibition of the initiation/propagation process of pitting can occur as follow:



The presence of NH₄⁺ ions precipitate in repassivation process on metallic surface.

The present work aims to apply coating of neodymium doped titanium on SS 316L by DC sputtering to investigate the electrochemical properties, where the Nd metal was doped as neodymium nitrate to implantation some benefited metals (Nd, N and Ti) with steel surface in order to test the corrosion in simulated body fluid at 37°C.

2. Experimental procedure

2.1 Materials

Samples of SS 316L were used as substrate to deposit Nd/Ti coating on them; the chemical composition is listed in Table 1. The grinding with SiC papers was done on square specimens with dimension of (20×20×5 mm) by sequence of (600, 800, 1000, and 1200 grit size) followed by polishing with alumina paste.

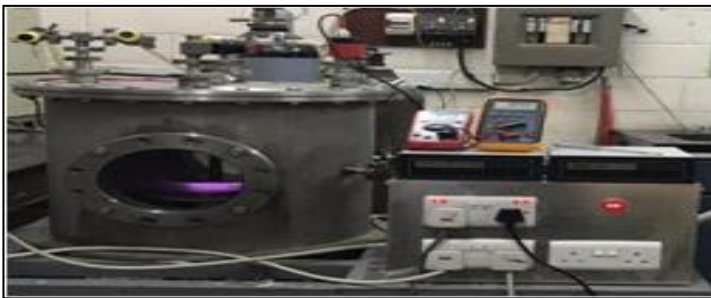
Table 1: Chemical composition of used stainless steel

<i>Metal</i>	<i>C</i>	<i>P</i>	<i>Si</i>	<i>Mn</i>	<i>S</i>	<i>Mo</i>	<i>Cr</i>	<i>Ni</i>	<i>Cu</i>	<i>Fe</i>
<i>Wt%</i>	0.022	0.031	0.407	1.43	0.004	2.00	16.98	11.73	0.234	Rem.

2.2 Coating process

To apply coating by DC sputtering, disk of stainless steel as anode and plasma source as cathode were used and with DC power supply of (4 kV) under Argon (Ar) atmosphere. Experimental conditions were: (4 h) as deposition time, (9 × 10⁻² mbar) as work pressure, (1 × 10⁻⁴ mbar) as initial pressure, (1250 V) as voltage and (20 mA) as electrical

current [8] (See Fig. 1, a). Titanium (Purity 98.5%, Fluka chemi AGCH-9470 Buckes) with neodymium nitrate Nd (NO₃)₃.6H₂O (Purity >99%, Chemacraft Ltd., Russia) were used with ration of (80:20) to prepare the target as disk with dimensions of (diameter 50 mm and thickness 5 mm). Image of coated sample can be seen in Fig. 1, b.



a)



b)

Figure 1. a) DC sputtering device, b) coated sample

2.3 Characterization methods

The structural and formed phases were studied using an XRD analysis with CuK α radiation (1.5418 Å) made in China, 2700A, HAOYUAN Co. SEM/EDS examination was taken using scanning electron microscope

(SEM) (FEI Quata 250, Czech Republic) and the surface morphology of the deposited coating was recorded using an Atomic Force Microscope (AFM) (NaioAFM 2022 nanosufr, Switzerland, and ultrasharp gold tip), see Fig. 2.

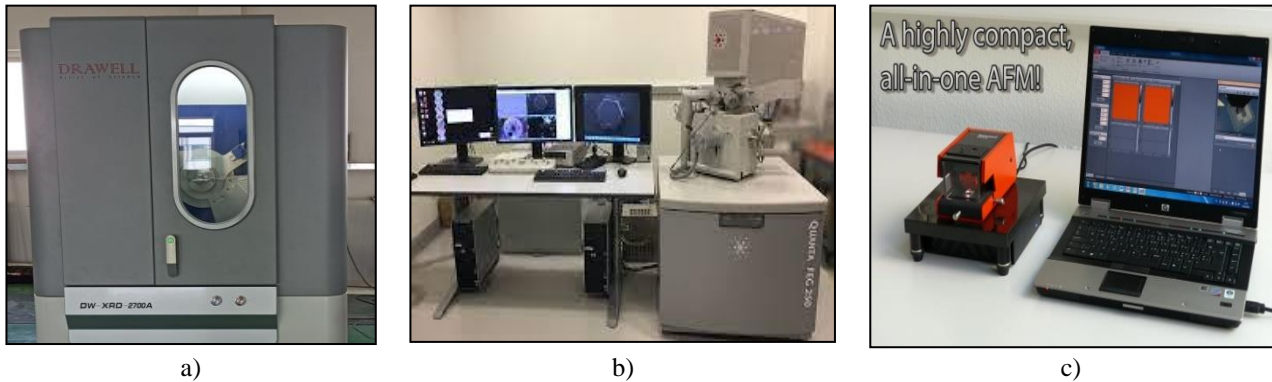


Figure 2. Devices of characterization; a) XRD, b) SEM and c) AFM

2.4 Corrosion measurement

The electrochemical properties were measured by recording open circuit potential (OCP), and Tafel plots for uncoated and coated samples using cell with three electrodes represented by saturated Calomel electrode (SCE) as reference, Pt electrode as counter, and SS 316L samples as working in Ringer Lactate medium (Pharmaceutical Solution Industry) after adjusting pH by sodium bicarbonate. All test were carried out at 37°C using Compactstat (Potentiostat/ galvanostat), Ivium with controlled software, Fig. 3.



Figure 3. Potentiostat

3. Results and discussion

3.1 Characterization of coated surface

XRD pattern of thin film deposited SS 316L (Fig. 4) shows the diffraction peaks related to mainly crystalline phase of stainless steel (316 L) according to (JCPDS card No. 33-0397) that appear at $2\theta = 43.604^\circ, 50.769^\circ$ and 74.65197° . Because of thin coating layer, the peaks of coating are weak compared with the peaks of substrate and also incorporated with them such as the peak at $2\theta = 40.170^\circ$ for Ti according to (JCPDS card No. 44-1294), at $2\theta = 41.710^\circ, 35.906^\circ$ and 60.448° for TiC according to (JCPDS card No. 32-1383), at $2\theta = 34.128^\circ, 39.311^\circ$ and 42.653° for Nd according to (JCPDS card No. 39-0914), and at $2\theta = 50.673^\circ$ for Nd₂O₃ according to (JCPDS card No. 40-1283), the standard and measured 2θ values with khl are listed in Table 2.

Table 2: The standard and measured of XRD data

2 θ / $^\circ$		khl
Standard	Measured	
43.582	43.5062	111
50.791	50.4878	200
74.697	74.4794	220

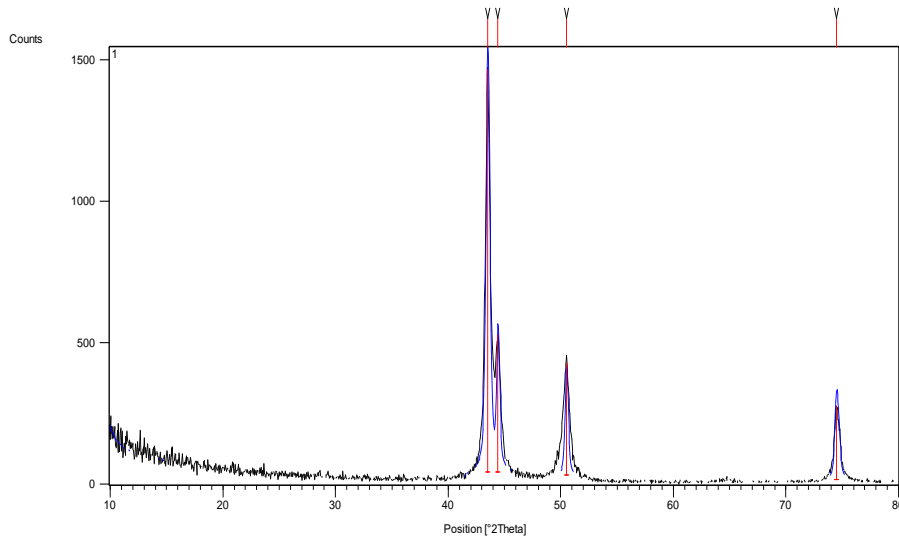


Figure 4. XRD pattern of coated SS 316L by Nd doped Ti coating

The structure and nature of deposited coating was investigated by scanning electron microscopy with EDS analysis. Fig. 5 shows the surface morphology of coating layer at two magnifications and these images indicate the strong columns with some particles distributed within these columns and some roughness correspond to a weaker character of columnar microstructure in the coating layer. These columns were observed by Shaha et al. when they studied the microstructure of thick (*TiC*) films grown by DC sputtering on smooth surface [9]. The white particles may attribute to neodymium metal as observed by Azadeh et al.

when they investigated the structure of Nd-TiO₂ layer that synthesized by the sol-gel method, and doped with Nd (NO₃)₃.6H₂O to increase the photocatalytic activity [10]. The EDS analysis in Fig. 6, indicates the ability of coating layer to isolate the substrate by decreasing the percent of main metals in stainless steel (Fe, Ni, Cr and Mn), while getting 16.02 wt% of Ti and 1.05 wt% of Nd as well as 18.99 and 52.44 wt% for oxygen and carbon respectively. The presence of oxygen is due to nitrate ions in neodymium nitrate, but the carbon is coming from steel to incorporate with coating metals. The distribution of these metals can be observed by mapping images as shown in Fig. 7.

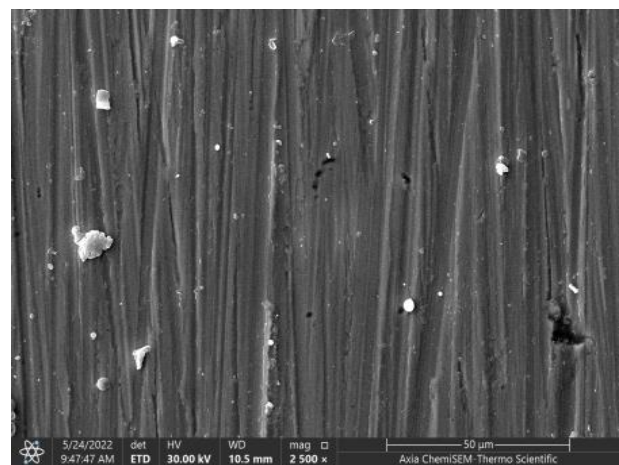
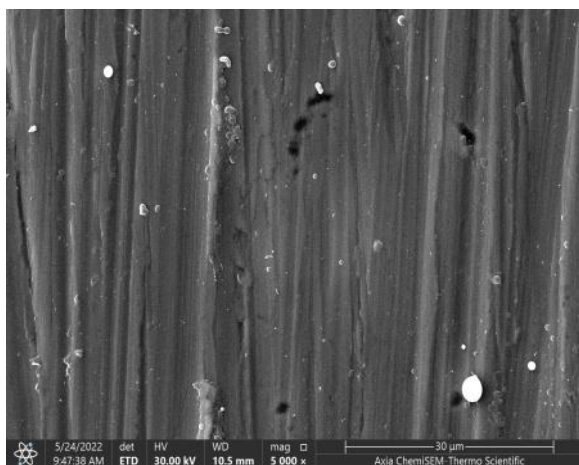


Figure 5. SEM images of Nd doped Ti coated SS 316L at two magnifications

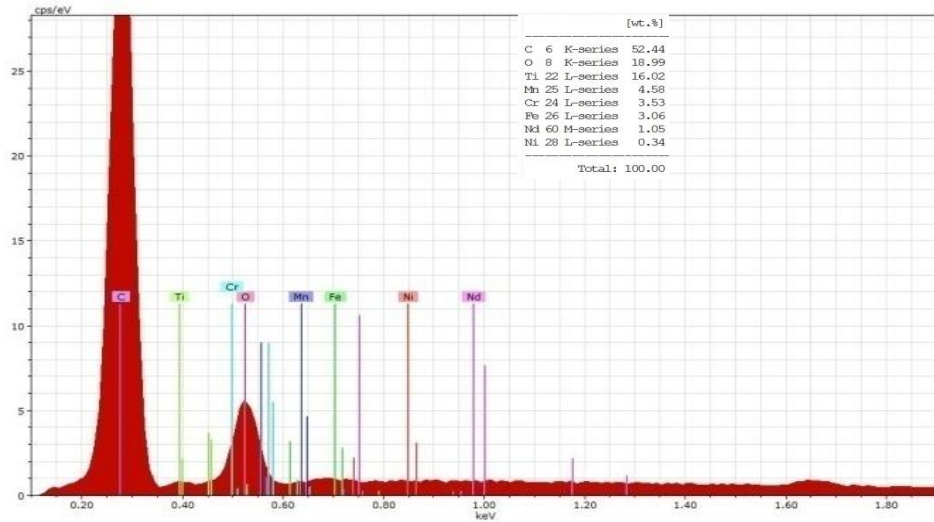


Figure 6. SEM/EDS exam of Nd doped Ti coated SS 316L

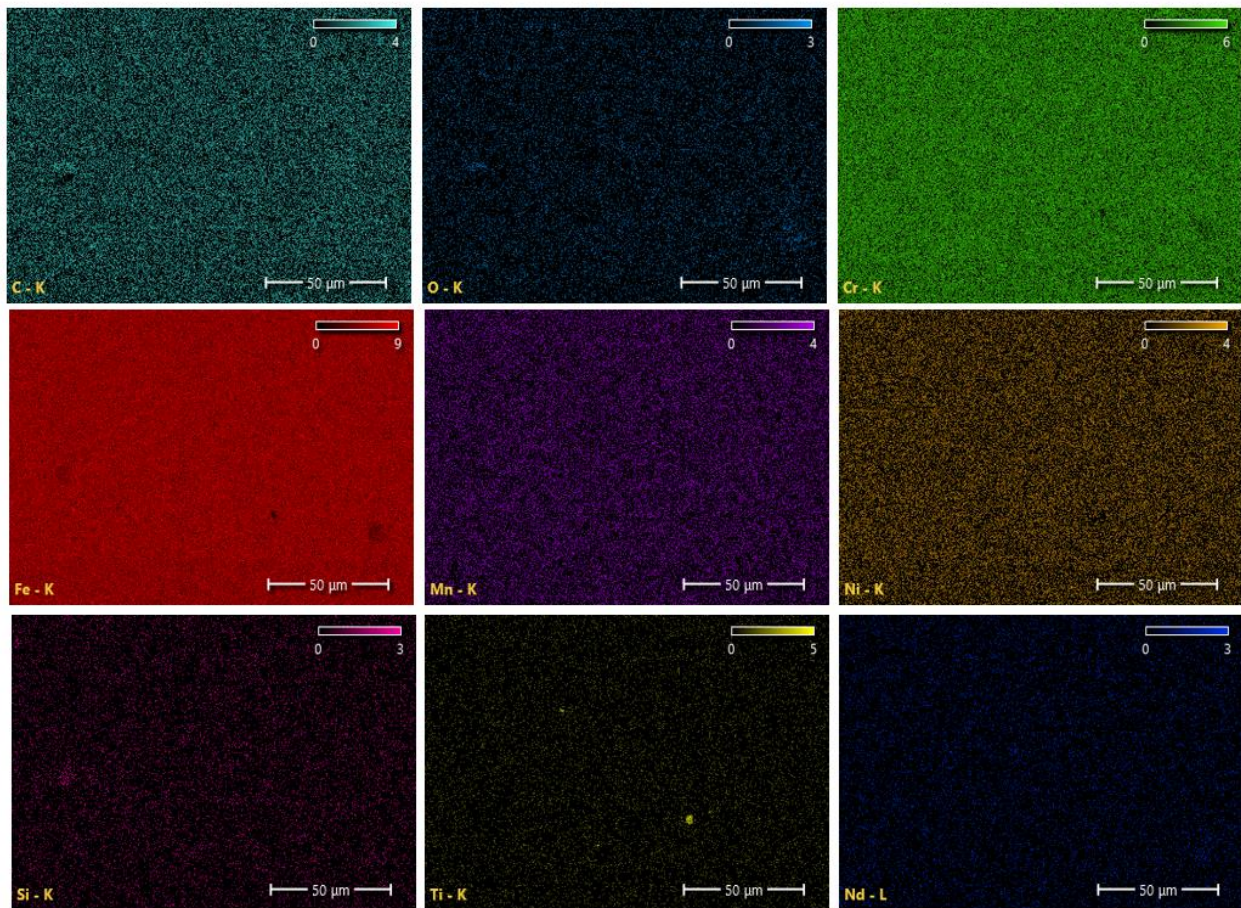


Figure 7. Mapping of Nd doped Ti coated SS 316L

The surface topography of uncoated and coated samples was investigated by AFM analysis by 2D and 3D images as shown in Fig. 8. This figure shows the more valleys and peaks in the images of coated sample significantly

affect the root-mean-square height (S_q) and the arithmetic mean height (S_a) values as listed in Table 3 with increasing surface roughness from 25.20 nm to 176.7 nm after coating.

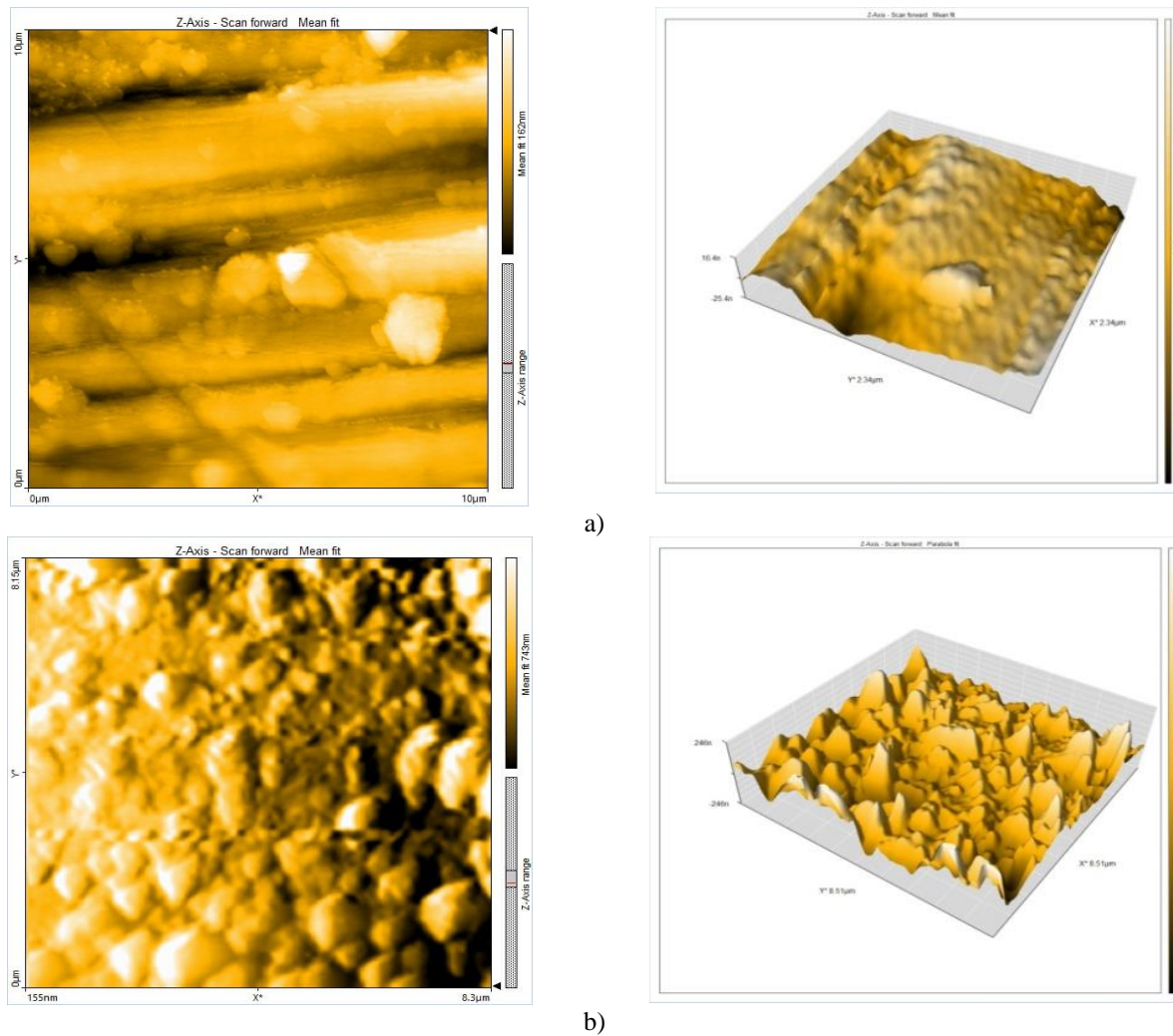


Figure 8. 2D and 3D of uncoated (a) and Nd doped Ti coated SS 316L (b) samples

Table 3: AFM data of uncoated and Nd doped Ti coated SS 316L samples

Parameter	Uncoated (nm)	Coated (nm)
Root-mean-square height (S_q)	32.08	238.2
Maximum peak height (S_p)	125.7	1379
Maximum pit depth (S_v)	81.84	873.5
Maximum height (S_z)	207.5	2252
Arithmetic mean height (S_a)	25.20	176.7

For deep analysis, the studying of surfaces morphology can be done with Abbott-Firestone curve which can simulate the theoretical wear effects and give information about the material and void volumes characterization [11, 12]. Fig. 9 shows the particles analysis and histogram for uncoated and coated samples, the histogram is the relation between number of values on y-axis and particle diameters on x-axis. The mean diameter was 710.8 nm and 362.8 nm for uncoated and coated surface respectively, while the number of particles were 123 and 192 respectively. The peak of roughness is defined

as the range of heights including (2– 25 %) of the bearing length while the medial and valley roughness are defined with (25– 75%) and (75– 98%) respectively [12] according to the standard DIN 4776 that depended on three zones classification of the Abbott-Firestone curve. In other papers [13, 14], the zoning of the Abbott-Firestone curve has five intervals as ($\leq 5\%$, 5– 10%, 10–50%, 50–95% and $\geq 95\%$). These results can be used to study the porous surfaces, where the 1st zone refers to the very high and prominent asperities that suffer from wear; the 2nd zone refers to the bearing and fluid retention

capabilities, also named micro-roughness and the 3rd zone. The 4th zone refers to the voids or the pores in the surface and the 5th zone has a level of depth to use as a criterion in evaluation the load capacity and wear resistance of a

surface. The range in coated sample is more than that for uncoated once, this means that the coated surface more resistant for wear than uncoated surface as well as the more roughness hinder the friction.

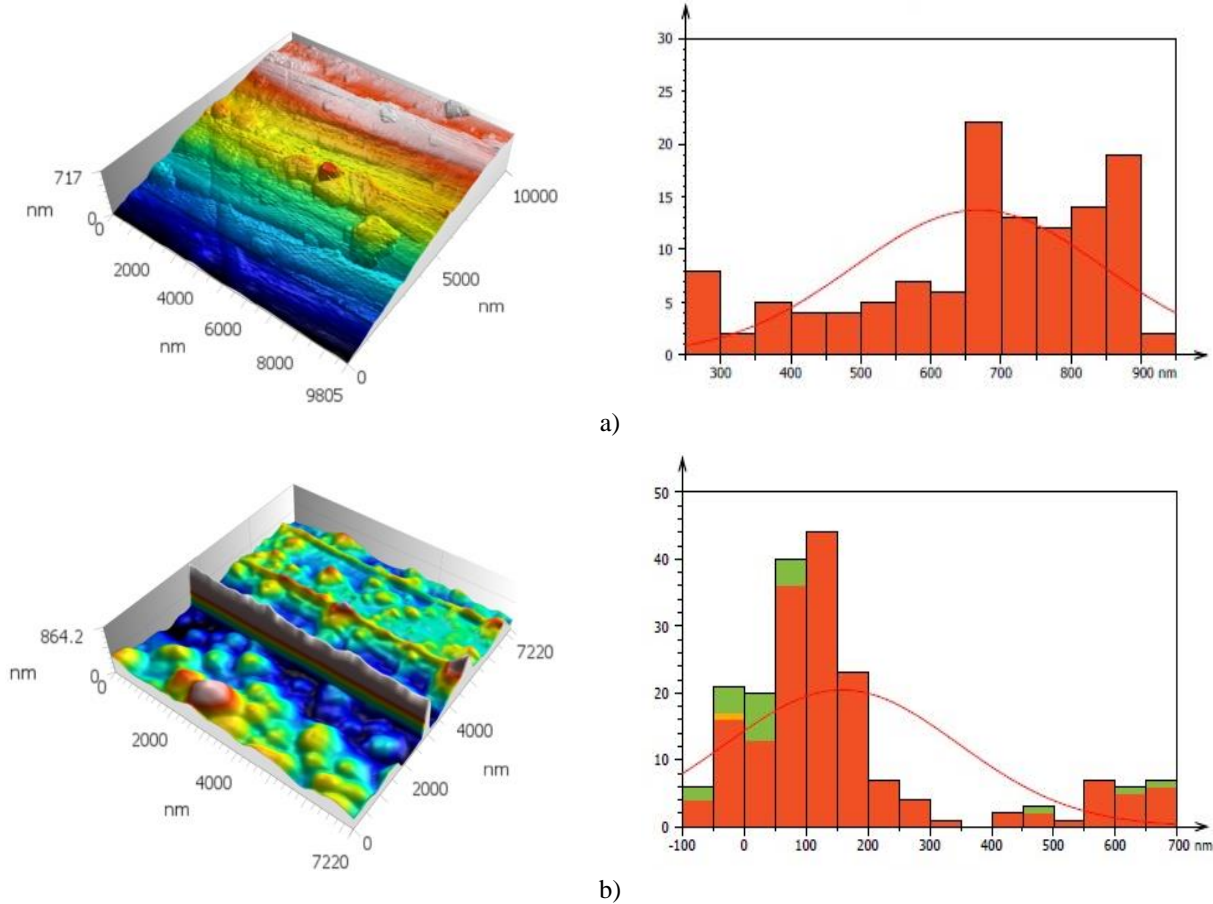
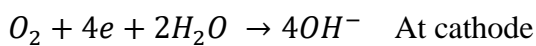
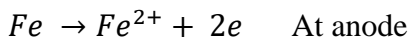


Figure 9. Particles analysis and histogram of uncoated (a) and Nd doped Ti coated SS 316L (b) samples

3.2 Electrochemical properties

Stainless steel corrodes in human body fluid according to the following reactions [15]:



Followed by formation of chromium oxide as passive film to protect the steel surface, but due to corrosivity of human body fluid, this passive film can be destroyed by harmful ions especially Cl^- and pitting will be occur rapidly. Applying the coating act as barrier to isolate the surface or prevent it from contact with environment. Nd/Ti coating was applied on SS 316L and the Figure 10 shows the Tafel plots of uncoated and coated samples. It is clear from

these curves (Plots) that the coating changed the cathodic and anodic behavior. At cathodic region, can be seen that the reaction is controlled by activation polarization rather than diffusion (concentration polarization). While at anodic region, there is a tendency to form passive films rather than for uncoated surface due to presence of titanium which form stable film of TiO_2 and the presence of neodymium which form Nd_2O_3 film. The data of corrosion are listed in Table 4, that refer to shifting corrosion potential (E_{corr}) to more positive value (+32.7 V) compared with potential of uncoated sample (-67.6 V) and decreasing the corrosion current density (i_{corr}).

Cathodic and anodic Tafel slopes (b_c & b_a) were decreased after coating, these slopes can be

used to calculate polarization resistance (R_p) as follow [16]:

$$R_p = \frac{b_c \times b_a}{2.3 \times i_{corr}(b_c + b_a)} \quad (1)$$

The result shows the increasing of resistance after coating from (14.083×10^3) to (22.218×10^5). Also, protection efficiency ($PE\%$) can be calculated using the current

density for coated sample ($i_{corr,coated}$) and uncoated sample ($i_{corr,uncoated}$) as follow [17]:

$$PE\% = \left[1 - \frac{i_{corr,coated}}{i_{corr,uncoated}} \right] \times 100 \quad (2)$$

The efficiency gives 97.11% for Nd/Ti coating providing good barrier to protect the surface from dissolution.

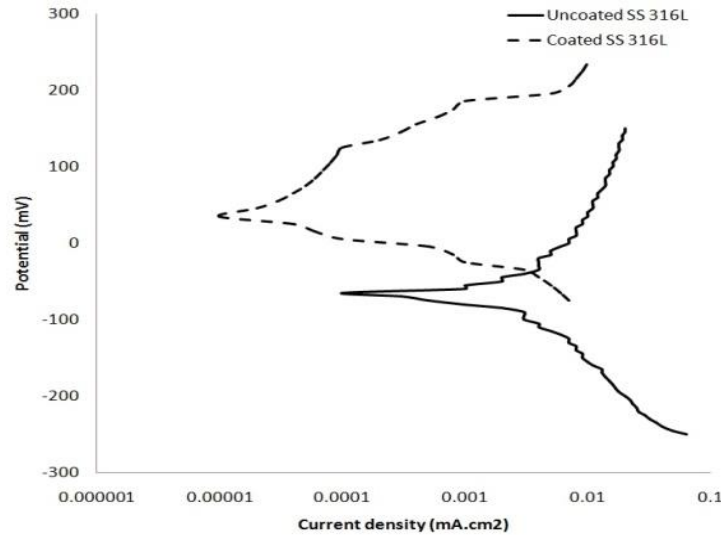


Figure 10. Polarization curves of uncoated and Nd doped Ti coated SS 316L

Table 4: Corrosion data of uncoated and Nd doped Ti coated SS 316L samples

Parameter	Uncoated	Coated
E_{corr} (V)	-67.6	+32.7
i_{corr} (mA.cm ⁻²)	1.535×10^{-6}	4.447×10^{-8}
$-b_c$ (V.dec ⁻¹)	0.097	0.047
$+b_a$ (V.dec ⁻¹)	0.102	0.044
C_R (mpy)	0.7019	0.02033
R_p (Ohm.cm ²)	14.083×10^3	22.218×10^5

4. Conclusions

The coating of Nd/Ti layer on stainless steel surface was successful by DC sputtering method to get compact insulated layer that consist of TiC and Nd₂O₃ as illustrated by XRD and SEM/EDS with more roughness (from 52.20 nm to 176.7 nm) due to difference in deposited metal particles as shown from AFM analysis. The investigation of corrosion behavior gave good results through shifting the potential toward noble direction (from -67.6 to +23.7 V) and decreasing current values (from 1.535×10^{-6} to 4.447×10^{-8} mA.cm⁻²) to obtain good protection efficiency equal to 97.11%.

References

- [1] S. Sedira, S. Achour, A. Avcı, V. Eskizeybek, "Physical deposition of carbon doped titanium nitride film by DC magnetron sputtering for metallic implant coating use", *Applied Surface Science*, vol. 295, pp. 81-85, 2014.
- [2] O. A. Fouada, R.A. Geioushy, S.M. El-Sheikh, M.H. Khedr, I.A. Ibrahim, "Metalorganic chemical vapor deposition of Ti–O–C–N thin films using TBOT as a promising precursor", *Journal of Alloys and Compounds*, vol. 509, pp. 6090-6095, 2011.
- [3] L. Fieandt, K. Johansson, E. Lindahl, T. Larsson, M. Boman, D. Rehnlund, "Corrosion properties of CVD grown Ti(C, N) coatings in 3.5 wt-% NaCl

- environment”, Corrosion Engineering, Science and Technology, vol. 53, pp. 316-320, 2018.
- [4] B. Burnat, P. Olejarz, D. Batory, M. Cichomski, M. Kaminska, D. Bociag, “Titanium dioxide coatings doubly-doped with Ca and Ag ions as corrosion resistant, Biocompatible, and Bioactive Materials for Medical Applications”, Coatings, vol. 10, pp.169, 2020.
- [5] R. Anae, A. Abdulkarim, M. Mathew, H. Jedy, “The effect of Nb₂O₅/Ni coatings on the microstructural and corrosion behavior on carbon steel for marine application”, Journal of Bio- and Tribo-Corrosion, vol. 7, pp. 1, 2021.
- [6] H. Abdulaah, A. Al-Ghaban, R. Anae, “Deposition and characterization of Ca₃Ce (PO₄)₃ phase in coating to protect stainless steel 316L”, AIP Conference Proceedings, 2372, 040004, 2021.
- [7] H. Abdullah, A. Al-Ghaban, R. Anae, “Deposition of CeO₂/TCP thin film on stainless steel 316 L by RF sputtering”, Engineering and Technology Journal, vol. 39, pp. 625-631, 2021.
- [8] N. Najm, A. Ataiwi, R. Anae, “Annealing and coating influence on the mechanical properties, microstructure, and corrosion properties of biodegradable Mg alloy (AZ91)”, Journal of Bio- and Tribo-Corrosion, vol. 8, pp. 64, 2022.
- [9] K. Shaha, Y. Pei, C. Chen, A. Turkin, D. Vainshtein, J. De Hosson, “On the dynamic roughening transition in nanocomposite film growth”, Applied Physics Letters, vol. 95, pp. 223102, 2009.
- [10] A. Shamsikasmaei, M. Sohrabi, Sh. Dehaghi, H. Ghasemi, “Using the Taguchi optimization method for a Di-Azo dye by UV/Nd-TiO₂ and a fixed bed system”, Fresenius Environmental Bulletin, vol. 22, 2013.
- [11] W. Dong, “Comprehensive study of parameters for characterising three-dimensional surface topography. III: Parameters for characterising amplitude and some functional properties”, Wear, vol. 178, pp. 29-43, 1994.
- [12] Z. Stamboliska, M. Kuzinovski, “Analysis and Mathematical Interpretation of Parameters That Describe the Microstereometry of Machined Surfaces” 3th Inter. Conf. of Tribology, I, 1999, pp. 21-28.
- [13] P. Kjeldsteen, “Wear resistance of PM materials and its dependency on surface topography”, Procs of Powder Metallurgy World Congress, vol. 1, pp. 657-660, 1994.
- [14] P. Kjeldsteen, “Tribological investigations of P/M Stainless steels mixed with HCX23 against Al₂O₃ & SiC”, Danfoss Research Report MUP2 (1997).
- [15] E. Yaqo, R. Anae, M. Abdulmajeed, I. Tomi, M. Kadhim, “Electrochemical, morphological and theoretical studies of an oxadiazole derivative as an anti-corrosive agent for kerosene reservoirs in Iraqi refineries”, [Chemical Papers](#), vol. 74, pp. 1739-1757, 2020.
- [16] N. Najm, A. Ataiwi, R. Anae, “Effect of indium coating on corrosion behavior of AZ31 Mg alloy by DC sputtering”, Materials Today: Proceedings, vol. 62, pp. 4551-4555, 2022.
- [17] H. Abdullah, R. Adnan, R. Anae, “Deposition of CaO to protect carbon steel by electrophoretic method”, Materials Today: Proceedings, vol. 26, pp. 4556-4561, 2022.